INTERNATIONAL JOURNAL FOR NUMERICAL METHODS IN ENGINEERING
Int. J. Numer. Meth. Engng (2014)
Published online in Wiley Online Library (wileyonlinelibrary.com). DOI: 10.1002/nme.4779

A decomposition-based approach to uncertainty analysis of feed-forward multicomponent systems

Sergio Amaral, Douglas Allaire and Karen Willcox*,†

Department of Aeronautics and Astronautics, Massachusetts Institute of Technology, Cambridge, MA 02139, USA

SUMMARY

To support effective decision making, engineers should comprehend and manage various uncertainties throughout the design process. Unfortunately, in today's modern systems, uncertainty analysis can become cumbersome and computationally intractable for one individual or group to manage. This is particularly true for systems comprised of a large number of components. In many cases, these components may be developed by different groups and even run on different computational platforms. This paper proposes an approach for decomposing the uncertainty analysis task among the various components comprising a feed-forward system and synthesizing the local uncertainty analyses into a system uncertainty analysis. Our proposed decomposition-based multicomponent uncertainty analysis approach is shown to be provably convergent in distribution under certain conditions. The proposed method is illustrated on quantification of uncertainty for a multidisciplinary gas turbine system and is compared to a traditional system-level Monte Carlo uncertainty analysis approach. Copyright © 2014 John Wiley & Sons, Ltd.

Received 2 October 2013; Revised 3 July 2014; Accepted 6 August 2014

KEY WORDS: uncertainty propagation; uncertainty analysis; importance sampling; multidisciplinary; multicomponent; decomposition; MDO

NOMENCLATURE

d_m	Number of inputs to Component m
f_m	Input-output function associated with Component m
K	Kernel function
k_m	Number of outputs of Component m
L	Bandwidth parameter in kernel density estimation
n_{eff}	Effective sample size
P	Proposal distribution function
P^n	Proposal empirical distribution function
p	Proposal density function
Q	Target distribution function
Q^n	Weighted proposal empirical distribution function
$\mathcal{Q}_m^n$	Random variable with distribution function Q^n
q	Target density function
t	Integration variable
w	Importance sampling weights
$\mathbf{x}$	Vector of system variables

*Correspondence to: Karen E. Willcox, Department of Aeronautics and Astronautics, Massachusetts Institute of Technology, Cambridge, MA 02139, USA.
†E-mail: kwillcox@mit.edu

$\mathbf{x}_{\mathcal{I}_m}$	Vector of variables with indices in the set $\mathcal{I}_m$
$\mathbf{x}_{\mathcal{J}_m}$	Vector of variables with indices in the set $\mathcal{J}_m$
$\mathbf{x}_{\mathcal{K}_m}$	Vector of variables with indices in the set $\mathcal{K}_m$
$\mathbf{x}_{\mathcal{O}_m}$	Vector of variables with indices in the set $\mathcal{O}_m$
$\mathbf{x}_{\mathcal{S}_m}$	Vector of variables with indices in the set $\mathcal{S}_m$
$\mathbf{x}_{\mathcal{T}_m}$	Vector of variables with indices in the set $\mathcal{T}_m$
$\mathbf{x}_{\mathcal{U}_m}$	Vector of variables with indices in the set $\mathcal{U}_m$
$\mathbf{x}_{\mathcal{V}_m}$	Vector of variables with indices in the set $\mathcal{V}_m$
$\mathbf{Y}_m$	Random vector of inputs to Component m
$\mathbf{y}_m$	Vector of inputs to Component m
$\mathcal{D}_m$	Domain of integration for Component m
$\mathcal{I}_m$	Set of indices of the system variables that are inputs to Component m
$\mathcal{J}_m$	Set of indices of all of the inputs and outputs associated with the first $m-1$ components, as well as the indices of the system inputs of Component m
$\mathcal{K}_m$	Set of indices in $\mathcal{J}_m$ with the exception of those indices in $\mathcal{I}_m$
$\mathcal{M}_i$	ith set of components
$\mathcal{O}_m$	Set of indices of the outputs of Component m
$\mathcal{S}_m$	Set of indices of new system inputs to Component m
$\mathcal{T}_m$	Set of indices of the shared inputs of Component m with any of the previous $m-1$ components' inputs or outputs
$\mathcal{U}_m$	Set of indices of the inputs and outputs of the first m components
$\mathcal{V}_m$	Set of indices of the inputs and outputs of Component m
Π	Generic distribution function
π	Generic density function
$\hat{\pi}$	Estimate of a density function, π
$\mathbf{1}$	Indicator function

1. INTRODUCTION

Multidisciplinary analysis is an extensive area of research, intended to support today's modern engineered systems, which are designed and developed by multiple teams. In addition to the difficulties associated with the design of such systems, the need to enhance performance and efficiency often drives the design to its physical limits. Therefore, the current methodology of modeling a baseline scenario and taking into account safety factors may no longer be sufficient. Instead, a rigorous characterization and management of uncertainty is needed, using quantitative estimates of uncertainty to calculate relevant statistics and failure probabilities. The estimation of these quantities requires an uncertainty analysis of the entire system. However, uncertainty analysis of the entire system may be cumbersome because of factors that result in inadequate integration of engineering disciplines, subsystems, and parts, which we refer to collectively here as *components*. Such factors include components managed by different groups, component design tools or groups housed in different locations, component analyses that run on different platforms, components with significant differences in analysis run times, lack of shared expertise among groups, and the sheer number of components comprising the system.

This paper proposes a different vision for system uncertainty analysis—decomposition of the multicomponent uncertainty analysis task, performing uncertainty analysis on the respective components individually, and assembling the component-level uncertainty analyses to quantify the system uncertainty analysis. We propose a rigorous methodology with guarantees of convergence in distribution, inspired by decomposition-based multidisciplinary optimization methods [1–4]. This paper specifically considers the problem of propagating uncertainty through a feed-forward multicomponent system to quantify the uncertainty of the system outputs of interest.

The challenges of system uncertainty analysis, illustrated on the left in Figure 1, often lie in integrating the components and in the computational expense of simulating the full system.

DOI: 10.1002/nme

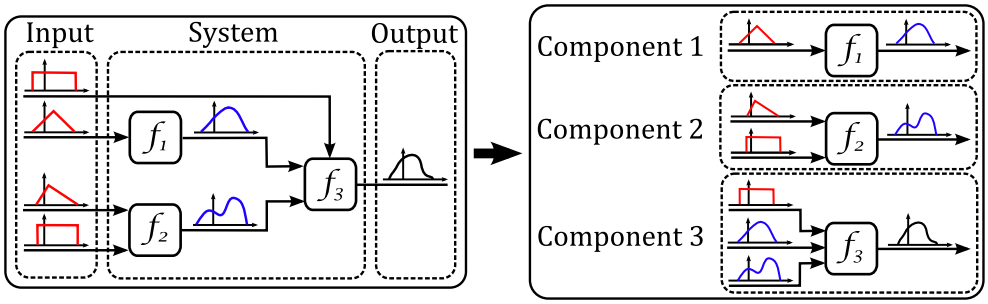

Figure 1. The proposed method of multicomponent uncertainty analysis decomposes the problem into manageable components, similar to decomposition-based approaches used in multidisciplinary analysis and optimization, and synthesizes the system uncertainty analysis without needing to evaluate the system in its entirety.

Past work has tackled these challenges through the use of surrogate modeling and/or a simplified representation of system uncertainty. Using surrogates in place of the higher fidelity components in the system provides computational gains and also simplifies the task of integrating components [5]. Using a simplified uncertainty representation (e.g., using mean and variance in place of full distributional information) avoids the need to propagate uncertainty from one component to another. Such simplifications are commonly used in uncertainty-based multidisciplinary design optimization methods as a way to avoid a system-level uncertainty analysis (see e.g., [6] for a review of these methods and their engineering applications). Such methods include implicit uncertainty propagation [7], reliability-based design optimization [8], moment matching [9], advanced mean value method [10], collaborative reliability analysis using most probable point estimation [11], and a multidisciplinary first-order reliability method [12].

Recent methods have exploited the structure of the multicomponent system to manage the complexity of the system uncertainty analysis. A likelihood-based approach has been proposed to decouple feedback loops, thus reducing the problem to a feed-forward system [13]. Dimension reduction and measure transformation to reduce the dimensionality and propagate the coupling variables between coupled components have been performed in a coupled feedback problem with polynomial chaos expansions [14–16]. Multiple models coupled together through a handful of scalars, which are represented using truncated Karhunen-Loève expansions, have been studied for multiphysics systems [17]. A hybrid method that combines Monte Carlo sampling and spectral methods for solving stochastic coupled problems has also been proposed [18, 19]. The hybrid approach partitions the coupled problem into subsidiary subproblems, which use Monte Carlo sampling methods if the subproblem depends on a very large number of uncertain parameters and spectral methods if the subproblem depends on only a small or moderate number of uncertain parameters. Another method solved an encapsulation problem, without any probability information; upon acquiring probabilistic information, solution statistics of the epistemic variables were evaluated at the post-processing steps [20, 21].

Our approach tackles the complexity of uncertainty quantification in a multicomponent system through decomposition. As illustrated on the right in Figure 1, we decompose the system uncertainty analysis into individual component-level uncertainty analyses that are then assembled in a provably convergent manner to the desired system uncertainty analysis. Many benefits that were not present in the previous works are gained through decomposing the system uncertainty analysis. Such benefits include managing the system through divide and conquer, exploiting team disciplinary expertise, avoiding the challenges of tight analysis integration among components, and being consistent with many organizational structures.

The remainder of the paper is organized as follows. Section 2 presents background on the uncertainty analysis methods employed. In Section 3, we describe the algorithm including its technical elements. Section 4 provides the convergence analysis and presents an *a posteriori* indicator to assess the effects of the assumptions underlying the decomposition. In Section 5, we present the results on an aerospace system application problem. Finally, conclusions are drawn in Section 6.

DOI: 10.1002/nme

2. PROBLEM STATEMENT

Uncertainty analysis is the process of quantifying uncertainty in component outputs that arise from uncertainty in component inputs [22], sometimes referred to as forward propagation of uncertainty. Computational methods for component uncertainty analysis can be classified into two groups: intrusive and non-intrusive techniques. Intrusive approaches require access to the existing computational components, which may not always be possible. Non-intrusive approaches, also known as sampling-based methods, do not require modification of existing computational components and instead treat the components as a 'black-box'. This paper focuses on sampling-based methods and in particular pseudorandom Monte Carlo simulation, due to its broad applicability.

As shown in Figure 1, we wish to perform system uncertainty analysis by propagating uncertainty in system inputs to uncertainty in system outputs. We aim to do this by performing uncertainty analyses on system components in a local 'offline phase' (ahead of time, decoupled from other component analyses) followed by a synthesis of the component-level analyses in an 'online phase'. This online synthesis step should ensure that system uncertainty analysis results are achieved in a provably convergent manner, while avoiding any evaluations of the system in its entirety. Specifically, our goal is to develop a decomposition-based uncertainty analysis methodology where the quantities of interest estimated from our decomposition-based approach converge in distribution to the true quantities of interest of the integrated feed-forward system.

Definition 1
A system is a collection of M coupled components. Each component has an associated function that maps component input random variables to component output random variables. Let $\mathbf{x} = (x_1, x_2, \ldots, x_d)^T$ be the vector of system variables, composed of the inputs and outputs of each component of the system, where shared inputs are not repeated in the vector. For Component m, where $m \in \{1, 2, \ldots, M\}$, let $\mathcal{I}_m \subset \{1, 2, \ldots, d\}$ denote the set of indices of the system variables corresponding to inputs to Component m and let $\mathcal{O}_m \subset \{1, 2, \ldots, d\}$ denote the set of indices corresponding to the outputs from Component m. Define $d_m = |\mathcal{I}_m|$ and $k_m = |\mathcal{O}_m|$. We denote the function corresponding to Component m as $f_m : \mathbb{R}^{d_m} \to \mathbb{R}^{k_m}$, which maps that component's random input vector, $\mathbf{X}_{\mathcal{I}_m} : \Omega \to \mathbb{R}^{d_m}$, where Ω is the product sample space of the input random vector, into that component's random output vector, $\mathbf{X}_{\mathcal{O}_m} = f_m(\mathbf{X}_{\mathcal{I}_m})$. A system whose components can be labeled such that the inputs to the i^{th} component can be outputs from the j^{th} component only if $j < i$ is a feed-forward system.

For a feed-forward system, a system-level Monte Carlo uncertainty analysis propagates uncertainty through the system's components by propagating realizations of the random inputs to the system in a serial manner. That is, realizations are propagated through the system on a component-by-component basis, requiring components with outputs that are inputs to downstream components to be run prior to running downstream components. This can be problematic if components are housed in different locations or owned by different groups, due to communication challenges and the possible transfer of large datasets. Furthermore, any changes to upstream components (e.g., modeling changes and changes in input uncertainty distributions) will require re-computing all downstream uncertainty analyses. The next section describes our proposed methodology to address these challenges, by decomposing the system-level uncertainty analysis into a set of offline local uncertainty analyses at the component level.

3. DECOMPOSITION-BASED MULTICOMPONENT UNCERTAINTY ANALYSIS

This section first presents an overview of our approach, and then describes the methodological ingredients of importance sampling and density estimation. We then describe the details of an essential element contributed by our approach: accounting for dependencies among system variables.

DOI: 10.1002/nme

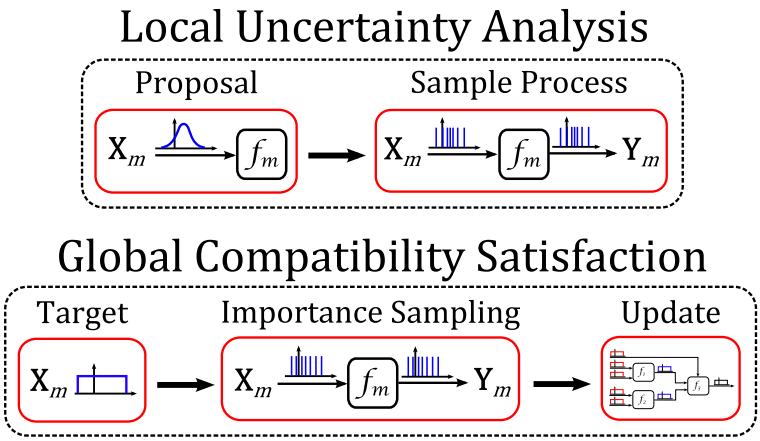

Figure 2. The process depicts the local uncertainty analysis and global compatibility satisfaction for Component m. First, local uncertainty analysis is performed on the component. Second, global compatibility satisfaction uses importance sampling to update the proposal samples so as to approximate the target distribution. Finally, an update step accounts for dependence among variables.

3.1. Overview of multicomponent uncertainty analysis

Our proposed decomposition-based multicomponent uncertainty analysis approach comprises two main procedures: (1) local uncertainty analysis: perform a local Monte Carlo uncertainty analysis on each component using their respective proposal distributions; and (2) global compatibility satisfaction: resolve the coupling among the components *without any further evaluations of the components or of the system as a whole*. Figure 2 represents the local and global steps of our approach for a generic component.

Each local uncertainty analysis is carried out in a decoupled offline phase. The challenge created by decomposition is that the distribution functions of the inputs for each component are unknown when conducting the local uncertainty analysis. Therefore, we propose an initial distribution function for each component input, which we refer to as the *proposal distribution function*. Local uncertainty analysis uses the proposal distribution function to generate samples of the uncertain component inputs and propagate them through the component analysis to generate corresponding samples of component outputs.

In the online phase, we learn the true distribution function of the inputs of each component. We refer to these true distribution functions as the *target distribution functions*. For those component inputs that correspond to system inputs, the target distribution functions represent the particular specified scenario under which we wish to perform the system uncertainty analysis. For those component inputs that correspond to coupling variables (i.e., they are outputs from upstream components), the target distribution functions are specified by the uncertainty analysis results of the corresponding upstream component(s).

Global compatibility satisfaction is ensured by starting with the most upstream components of the system and approximating their respective target distribution functions using importance sampling on the corresponding proposal distribution functions. The densities of updated output samples of these components are then represented using density estimation. We construct joint densities among the inputs and outputs of these upstream components to account for any dependencies that were not captured in the marginal densities of each component's outputs. Once this is complete, downstream components receive their respective target distribution functions, and the process of importance sampling and accounting for dependence is repeated through the system.

The theoretical analysis presented in Section 4 requires that components can be represented by piecewise functions each of which are one-to-one and continuously differentiable on sets of finite measure. In addition, the density estimation steps of the approach will suffer loss of accuracy if the underlying densities are not sufficiently smooth. This restricts the class of problems for which we can expect good convergence of the decomposition-based approach. For smooth problems,

DOI: 10.1002/nme

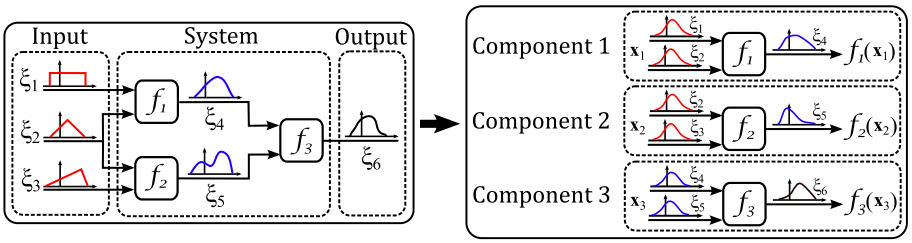

Figure 3. Three components of a feed-forward system shown from the system Monte Carlo perspective (left) along with the same components exercised concurrently from the perspective of the decomposition-based multicomponent uncertainty analysis (right).

methods such as stochastic Galerkin and stochastic collocation can yield faster convergence than Monte Carlo simulation for problems of moderate dimension. In this paper, we set up our mathematical framework using Monte Carlo simulation, due to its broader generality; while we do not develop the theory here, our general approach of decomposing into local uncertainty analysis and global compatibility satisfaction could also be combined with stochastic Galerkin and stochastic collocation methods. We also note that if importance weights could be computed without requiring density estimation (the subject of our ongoing work), then our decomposition approach will be applicable to a more general class of multidisciplinary engineering problems, including those that exhibit irregular dependencies, steep gradients, and sharp transitions.

To describe our decomposition-based approach more concretely, we consider the specific case of a three-component feed-forward system, shown in Figure 3, although our approach extends to multiple components and other forms of component feed-forward coupling. The system inputs are $(\xi_1, \xi_2, \xi_3)^T$, and ξ_6 is the system output quantity of interest. The coupling variable ξ_4 is an output of Component 1 and an input of Component 3, and the coupling variable ξ_5 is an output of Component 2 and an input of Component 3. Thus, the local uncertainty analysis for Component 1 involves evaluating f_1 with sample realizations of the proposal distribution functions of ξ_1 and ξ_2 in order to generate samples of ξ_4. Similarly, the local uncertainty analysis for Component 2 involves evaluating f_2 with sample realizations from the proposal distribution functions of ξ_2 (independent of the samples of ξ_2 drawn for Component 1) and ξ_3, to generate samples of ξ_5, and the local uncertainty analysis of Component 3 involves the evaluation of f_3 with sample realizations from proposal distribution functions of ξ_4 and ξ_5 to generate samples of ξ_6. The key challenges in decomposing the uncertainty analysis for this system are as follows: (1) the local Monte Carlo simulation for f_3 is performed before the target distribution function of the coupling variables ξ_4 and ξ_5 is known, and (2) the dependence between ξ_4 and ξ_5 due to ξ_2 is not accounted for in the local analyses.

Starting from the upstream components, here Component 1 and Component 2, importance sampling assigns weights to the computed samples so as to approximate the input target distribution functions of each component using the samples previously simulated during local analysis from the input proposal distribution functions. The result is an updated output target marginal distribution function of ξ_4 and ξ_5 that requires no further evaluations of the Component 1 or Component 2 functions. To account for the dependence between ξ_4 and ξ_5, we construct the joint density of $(\xi_4, \xi_5)^T$ using a conditioning process that is described in detail in Section 3.5 and again requires no further evaluations of the component functions. We then use importance sampling for Component 3 to yield an updated output target distribution function for ξ_6. As a result, the system input target distribution functions are propagated downstream to quantify the distribution function of the output quantity of interest, here ξ_6, without having to perform a full system-level uncertainty analysis. As shown in Section 4.1, under some mild assumptions on the component functions, the results of the decomposition-based approach converge in distribution to the true variables of the feed-forward system.

DOI: 10.1002/nme

3.2. Local uncertainty analysis

To simplify notation in the presentation of the local analysis for Component m, we define $\mathbf{y}_m = \mathbf{x}_{\mathcal{I}_m}$, the vector of inputs to Component m. We define the proposal distribution function for the inputs of Component m as

$$P(\mathbf{y}_m) = \int_{\mathcal{D}_m} p(\mathbf{t})\, \mathrm{d}\mathbf{t}, \tag{1}$$

where $\mathbf{y}_m = (y_{m,1}, y_{m,2}, \ldots, y_{m,d_m})^T$, $p(\mathbf{y}_m)$ is the proposal density of the input random vector, $\mathbf{Y}_m = (Y_{m,1}, Y_{m,2}, \ldots, Y_{m,d_m})^T$, and $y_{m,j}$ denotes the j^{th} component of the vector $\mathbf{y}_m$. The domain of integration is $\mathcal{D}_m = (-\infty, y_{m,1}] \times (-\infty, y_{m,2}] \times \cdots \times (-\infty, y_{m,d_m})$, $\mathbf{t}$ is a dummy variable of integration, and we assume that the input random variables of each component are continuous. The local uncertainty analysis of Component m uses Monte Carlo simulation to generate n samples, $\{\mathbf{y}_m^i\}_{i=1}^n$, from the proposal distribution function $P(\mathbf{y}_m)$, where $\mathbf{y}_m^i$ denotes the i^{th} sample. We propagate those samples through the component, computing the corresponding component outputs $\{f_m(\mathbf{y}_m^i)\}_{i=1}^n$.

The proposal distribution function $P(\mathbf{y}_m)$ represents our 'best guess' at describing the uncertainty in the inputs of Component m, made before we receive distributional information from upstream components or system inputs. Choosing an appropriate proposal distribution is important but can be difficult because the target is unknown at the time the proposal is specified. The difficulties are that the target density must be absolutely continuous with respect to the proposal density, and at the same time, the proposal should adequately capture the dependence structure and high probability regions of the target. If the condition of absolute continuity is not satisfied, then the computation of the importance sampling weights (described in more detail in the next section) will fail. Therefore, it is typical to choose a conservative proposal distribution function, ensuring that the support of the proposal is sufficiently wide to encompass the full range of input values expected from upstream components or from system inputs. If the proposal has appropriate support, but does not adequately capture the structure of the target, then our convergence results in Section 4 still hold, but the number of samples needed in the offline stage (to achieve a desired accuracy level) may be prohibitive. The quality of the proposal distribution and its impact on the uncertainty assessment results are discussed in Section 4.2.

3.3. Sample weighting via importance sampling

We define the target distribution function of the inputs for Component m as

$$Q(\mathbf{y}_m) = \int_{\mathcal{D}_m} q(\mathbf{t})\, \mathrm{d}\mathbf{t}, \tag{2}$$

where $q(\mathbf{y}_m)$ is the target density of $\mathbf{Y}_m$. We use importance sampling to weight the pre-computed proposal samples, $\{\mathbf{y}_m^i\}_{i=1}^n$, ensuring that the weighted proposal input empirical distribution function converges pointwise to the target input distribution function.

Lemma 1
Let $Q^n(\mathbf{y}_m)$ be the weighted proposal empirical distribution function for the inputs to Component m, computed using n samples. We write

$$Q^n(\mathbf{y}_m) = \sum_{i=1}^{n} w(\mathbf{y}_m^i)\, \mathbf{1}_i(\mathbf{y}_m), \tag{3}$$

where $\mathbf{1}_i(\mathbf{y}_m)$ is the indicator function of the event $\left\{y_{m,j}^i \le y_{m,j}, \forall\, j \in \{1, 2, \ldots, d_m\}\right\}$, $w(\mathbf{y}_m^i) \propto \frac{q(\mathbf{y}_m^i)}{p(\mathbf{y}_m^i)}$ and subject to the condition that the weights sum to unity, and q is absolutely continuous with respect to p. Then

DOI: 10.1002/nme

$$\lim_{n\to\infty} Q^n(\mathbf{y}_m) = Q(\mathbf{y}_m), \tag{4}$$

where Q is the input target distribution function for Component m.

Proof
See, for example, Reference [23]. □

Lemma 1 shows that the weighted proposal input empirical distribution function converges to the input target distribution function. By applying Skorokhod's representation theorem and assuming that each $f_m(\mathbf{y}_m)$ is continuous, it is straightforward to show (see, e.g., [24]) that the corresponding empirical distribution of the component outputs converges to the distribution function of the target outputs. Thus, all that is required to ensure that we can change from proposal to target distribution functions for each component, without further model evaluations, is the ability to estimate the proposal and target input densities pointwise to provide the sample weights. We discuss how we accomplish this in the next section.

Algorithm 1 describes the importance sampling procedure. This process is shown notionally in Figure 4. The left plot in Figure 4 shows the contours, in solid, of an example proposal density and samples from that density as dots. Target density contours are shown on the same plot as the dashed curves. Importance sampling provides a weight for each red sample, where the relative weights of the samples are reflected by the size of the blue dots on the right plot of Figure 4.

We note here that if a poor proposal distribution function is selected, then the importance sampling algorithm may encounter sample impoverishment and therefore result in a poor convergence rate. Therefore, it is desirable to select a conservative proposal distribution function to account for the unknown target distribution function at the local uncertainty analysis step.

Algorithm 1: Importance Sampling for Component m.

Data: Target input distribution Q and density q, proposal distribution P and density p.
Result: Sample importance weight, $\{w^i\}_{i=1}^n$.
Sampling:
Generate n samples, $\{\mathbf{y}_m^1, \mathbf{y}_m^2, \ldots, \mathbf{y}_m^n\}$, i.i.d. from P;
Importance Sampling:
for $i \in \{1, \ldots, n\}$ **do**
  Assign to sample $\mathbf{y}^i$ the weight $w^i \propto \frac{q(\mathbf{y}_m^i)}{p(\mathbf{y}_m^i)}$;
end

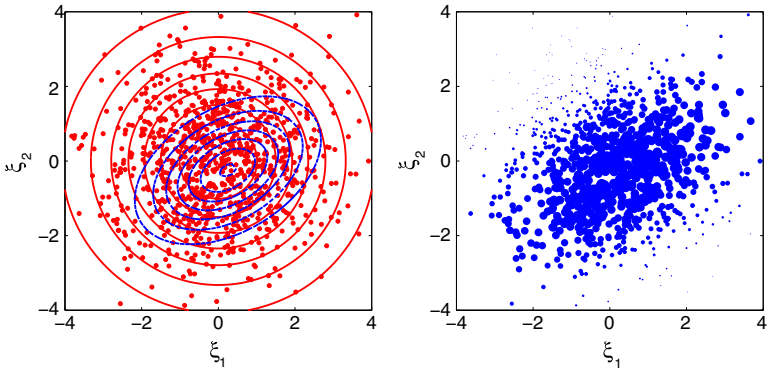

Figure 4. The importance sampling process uses the realizations (red dots on left figure) generated from a proposal distribution $P(\xi_1, \xi_2)$ (corresponding density shown as red solid contour on left figure) to approximate a target distribution $Q(\xi_1, \xi_2)$ (blue dash contour on left figure), by weighting the proposal realizations, (blue dots on right figure).

DOI: 10.1002/nme

3.4. Density estimation for estimating importance weights

Algorithm 1 computes importance weights that are the ratio of the target density to the proposal density for a given sample. Because we employ here a sample-based approach to uncertainty propagation, we require a means of estimating proposal and target densities from a set of samples. In particular for some continuous random variable Ξ with distribution function $\Pi(\xi)$ and a density $\pi(\xi)$, we require that for any density estimate, $\hat{\pi}(\xi)$,

$$\lim_{n\to\infty} \hat{\pi}(\xi) = \pi(\xi) \tag{5}$$

at all points of continuity of the density $\pi(\xi)$. For this, we use kernel density estimation,

$$\hat{\pi}(\xi) := \frac{1}{nL^d} \sum_{i=1}^{n} K\left(\frac{\xi - \xi^j}{L}\right), \tag{6}$$

where $L > 0$ is a bandwidth parameter with the property that $\lim_{n\to\infty} L = 0$ and K is a kernel function satisfying

$$0 \leqslant K(\mathbf{t}) \leqslant \infty, \tag{7}$$

$$\int_{\mathbb{R}^d} K(\mathbf{t})\, \mathrm{d}\mathbf{t} = 1, \tag{8}$$

$$\int_{\mathbb{R}^d} K(\mathbf{t})\xi\, \mathrm{d}\mathbf{t} = 0, \tag{9}$$

$$\int_{\mathbb{R}^d} K(\mathbf{t})\, ||\mathbf{t}||^2\, \mathrm{d}\mathbf{t} < \infty, \tag{10}$$

where $\mathbf{t} \in \mathbb{R}^d$ and $||\cdot||$ is the Euclidean norm. Then, $\lim_{n\to\infty} \hat{\pi}(\xi) = \pi(\xi)$ at every point ξ of continuity of $\pi(\cdot)$ [25, 26]. The Gaussian kernel function and mean integrated squared error bandwidth parameter selection criteria are implemented throughout all examples in this manuscript [27].

If the set of points of continuity of $\pi(\cdot)$ is of measure 1, then in the limit as $n \to \infty$, $\hat{\pi}(\xi)$ is a density of the distribution function $\Pi(\xi)$. To ensure this criterion, we require that the inputs to a given system be absolutely continuous random variables. Further, as discussed in Reference [24], the component functions, f_m, must be such that there are sets $\{I_1, I_2, \ldots, I_k\}$ that partition the component input space $\mathbb{R}^{d_m}$, such that $f_m : I_i \to \mathbb{R}^{k_m}$ is strictly one-to-one and continuously differentiable for each set i.

3.5. Accounting for dependence among variables

The weighting of samples via importance sampling in the global compatibility step of our multicomponent uncertainty analysis approach ensures that we achieve the target marginal distribution functions of a given component's inputs. However, the dependencies among variables, such as ξ_4 and ξ_5 in the system shown in Figure 3, are not captured. These dependencies must be recovered in order to achieve the correct results.

For example, consider again the system presented in Figure 3. The dependence between ξ_4 and ξ_5 caused by the common dependence on ξ_2 can be accounted for by considering the target density of $(\xi_4, \xi_5)^T$ and the dependence structure as follows [24]:

$$q(\xi_4, \xi_5) = \int_{\xi_2} q(\xi_2, \xi_4, \xi_5) d\xi_2 = \int_{\xi_2} q(\xi_2, \xi_4) \cdot q(\xi_5|\xi_2) d\xi_2 = \int_{\xi_2} \frac{q(\xi_2, \xi_4) \cdot q(\xi_2, \xi_5)}{q(\xi_2)} d\xi_2. \tag{11}$$

DOI: 10.1002/nme

Here, $q(\xi_2, \xi_4)$ is the target density associated with input ξ_2 and output ξ_4, which was constructed via importance sampling for Component 1. Likewise, $q(\xi_2, \xi_5)$ is the target density associated with input ξ_2 and output ξ_5, which was constructed via importance sampling for Component 2. We construct $q(\xi_4, \xi_5)$ using Equation (11), which uses the system's inherent dependence structure to yield the correct target input distribution function to Component 3.

To generalize the concept, consider the construction of the target density of the inputs to the first m components of an M-component feed-forward system, where the inputs to Component i cannot be the outputs of Component j unless $j < i$. Recall from Definition 1 that $\mathbf{x} = (x_1, x_2, \ldots, x_d)^T$ is the vector of system variables, $\mathcal{I}_m \subset \{1, 2, \ldots, d\}$ is the set of indices of the system variables corresponding to inputs to Component m, and $\mathcal{O}_m \subset \{1, 2, \ldots, d\}$ is the set of indices corresponding to the outputs from Component m. We further define $\mathcal{S}_m \subset \{1, 2, \ldots, d\}$ to be the set of indices of new system inputs to Component m, where new system inputs refer to those inputs that are not output from any component, are not inputs to any previous component, and are assumed independent. Then, let $\mathcal{V}_m = \mathcal{I}_m \cup \mathcal{O}_m$, which is the set of indices of the inputs and outputs of Component m, let $\mathcal{U}_m = \cup_{i=1}^{m} \mathcal{V}_m$, which is the set of indices of the inputs and outputs of the first m components, and let $\mathcal{T}_m = \left(\cup_{i=1}^{m-1} \mathcal{V}_i\right) \cap \mathcal{I}_m$, which is the set of indices of the shared inputs of Component m with any of the previous $m-1$ components' inputs or outputs. We also define $\mathcal{J}_m = \mathcal{U}_{m-1} \cup \mathcal{S}_m$, which is the set of indices of all of the inputs and outputs associated with the first $m-1$ components, as well as the indices of the system inputs of Component m, and let $\mathcal{K}_m = \mathcal{J}_m \setminus \mathcal{I}_m$. By constructing the target density of the variables with indices in the set $\mathcal{J}_m$, we correctly capture the dependence among the inputs to Component m. We denote by $\mathbf{x}_{\mathcal{J}_m}$ the vector of system variables corresponding to those indices in the set $\mathcal{J}_m$ (and similarly for the other sets defined previously).

For the example system given in Figure 3, with $m = 3$, we have that $\mathbf{x} = (\xi_1, \xi_2, \xi_3, \xi_4, \xi_5, \xi_6)^T$. The indices in each of the sets for $m = 1, 2$, and 3 are given in Table I. For this example, the target densities required for each component are $q\left(\mathbf{x}_{\mathcal{J}_1}\right) = q(\xi_1, \xi_2), q\left(\mathbf{x}_{\mathcal{J}_2}\right) = q(\xi_1, \xi_2, \xi_3, \xi_4)$, and $q\left(\mathbf{x}_{\mathcal{J}_3}\right) = q(\xi_1, \xi_2, \xi_3, \xi_4, \xi_5)$. The target densities, $q\left(\mathbf{x}_{\mathcal{J}_m}\right)$, contain the correct dependence structure for the inputs, $\mathbf{x}_{\mathcal{I}_m}$, to Component m. We write the target density of these inputs as $q\left(\mathbf{x}_{\mathcal{I}_m}\right)$ for each Component m. The evaluation of the input target density, $q\left(\mathbf{x}^i_{\mathcal{I}_m}\right)$, at proposal input samples, $\mathbf{x}^i_{\mathcal{I}_m}$, for each Component m, ensures that we can properly weight the proposal samples to each component of the system according to Algorithm 1.

Lemma 2

The target density of the inputs and outputs of the first $m-1$ components and the inputs to Component m, where $m \geqslant 3$, is given by

$$q\left(\mathbf{x}_{\mathcal{J}_m}\right) = \frac{\prod_{k=1}^{m-1} q\left(\mathbf{x}_{\mathcal{V}_k}\right)}{\prod_{l=2}^{m-1} q\left(\mathbf{x}_{\mathcal{T}_l}\right)} q\left(\mathbf{x}_{\mathcal{S}_m}\right), \tag{12}$$

where if $\mathcal{S}_m = \{\emptyset\}$, then $q\left(\mathbf{x}_{\mathcal{S}_m}\right) = 1$.

Table I. Index sets for the system presented in Figure 3.

$m = 1$	$m = 2$	$m = 3$
$\mathcal{I}_1 = \{1, 2\}$	$\mathcal{I}_2 = \{2, 3\}$	$\mathcal{I}_3 = \{4, 5\}$
$\mathcal{O}_1 = \{4\}$	$\mathcal{O}_2 = \{5\}$	$\mathcal{O}_3 = \{6\}$
$\mathcal{S}_1 = \{1, 2\}$	$\mathcal{S}_2 = \{3\}$	$\mathcal{S}_3 = \{\emptyset\}$
$\mathcal{V}_1 = \{1, 2, 4\}$	$\mathcal{V}_2 = \{2, 3, 5\}$	$\mathcal{V}_3 = \{4, 5, 6\}$
$\mathcal{U}_1 = \{1, 2, 4\}$	$\mathcal{U}_2 = \{1, 2, 3, 4, 5\}$	$\mathcal{U}_3 = \{1, 2, 3, 4, 5, 6\}$
$\mathcal{T}_1 = \{\emptyset\}$	$\mathcal{T}_2 = \{2\}$	$\mathcal{T}_3 = \{4, 5\}$
$\mathcal{J}_1 = \{1, 2\}$	$\mathcal{J}_2 = \{1, 2, 3, 4\}$	$\mathcal{J}_3 = \{1, 2, 3, 4, 5\}$
$\mathcal{K}_1 = \{\emptyset\}$	$\mathcal{K}_2 = \{1, 4\}$	$\mathcal{K}_3 = \{1, 2, 3\}$

DOI: 10.1002/nme

Proof

$$\frac{\prod_{k=1}^{m-1} q\left(\mathbf{x}_{\mathcal{V}_k}\right)}{\prod_{l=2}^{m-1} q\left(\mathbf{x}_{\mathcal{T}_l}\right)} q\left(\mathbf{x}_{\mathcal{S}_m}\right) = q\left(\mathbf{x}_{\mathcal{V}_1}\right) \frac{q\left(\mathbf{x}_{\mathcal{V}_2}\right)}{q\left(\mathbf{x}_{\mathcal{T}_2}\right)} \cdots \frac{q\left(\mathbf{x}_{\mathcal{V}_{m-1}}\right)}{q\left(\mathbf{x}_{\mathcal{T}_{m-1}}\right)} q\left(\mathbf{x}_{\mathcal{S}_m}\right) \tag{13}$$

$$= q\left(\mathbf{x}_{\mathcal{V}_1}\right) \frac{q\left(\mathbf{x}_{\mathcal{V}_2}\right)}{q\left(\mathbf{x}_{\mathcal{T}_2}\right)} \frac{\prod_{k=3}^{m-1} q\left(\mathbf{x}_{\mathcal{V}_k}\right)}{\prod_{l=3}^{m-1} q\left(\mathbf{x}_{\mathcal{T}_l}\right)} q\left(\mathbf{x}_{\mathcal{S}_m}\right) \tag{14}$$

$$= q\left(\mathbf{x}_{\mathcal{U}_2}\right) \frac{\prod_{k=3}^{m-1} q\left(\mathbf{x}_{\mathcal{V}_k}\right)}{\prod_{l=3}^{m-1} q\left(\mathbf{x}_{\mathcal{T}_l}\right)} q\left(\mathbf{x}_{\mathcal{S}_m}\right) \tag{15}$$

$$= q\left(\mathbf{x}_{\mathcal{U}_{m-1}}\right) q\left(\mathbf{x}_{\mathcal{S}_m}\right) \tag{16}$$

$$= q\left(\mathbf{x}_{\mathcal{J}_m}\right), \tag{17}$$

where Equation (15) follows from the definition of a conditional probability density (see, e.g., [24]) and Equation (17) follows because the system inputs of Component m are considered independent from all other system variables. □

Once we have the density $q\left(\mathbf{x}_{\mathcal{J}_m}\right)$, we can evaluate the input target density, $q\left(\mathbf{x}_{\mathcal{I}_m}\right)$, required by Component m with the correct dependence among the inputs. We note here that for a system with $m = 1$ component, there is no dependence structure to resolve. For $m \geqslant 2$, the input target density for Component m is given by

$$q\left(\mathbf{x}_{\mathcal{I}_m}\right) = \int_{\text{supp}\left(\mathbf{x}_{\mathcal{K}_m}\right)} q\left(\mathbf{x}_{\mathcal{K}_m}\right) q\left(\mathbf{x}_{\mathcal{J}_m} | \mathbf{x}_{\mathcal{K}_m}\right) \mathrm{d}\mathbf{x}_{\mathcal{K}_m}, \tag{18}$$

where $\text{supp}\left(\mathbf{X}_{\mathcal{K}_m}\right)$ is the support of the random vector $\mathbf{X}_{\mathcal{K}_m}$. We note here that Equation (18) is the expected value of the conditional density, $q\left(\mathbf{x}_{\mathcal{J}_m} | \mathbf{x}_{\mathcal{K}_m}\right)$ with respect to $q\left(\mathbf{x}_{\mathcal{K}_m}\right)$. The density $q\left(\mathbf{x}_{\mathcal{K}_m}\right)$ is obtained similarly to $q\left(\mathbf{x}_{\mathcal{J}_m}\right)$ using the densities in Equation (12) with the variables in $\mathbf{x}_{\mathcal{I}_m}$ marginalized out. The target input density, $q\left(\mathbf{x}_{\mathcal{I}_m}\right)$, only needs to be evaluated at the proposal samples as specified in Algorithm 1. A procedure for evaluating this density at the proposal samples, using Monte Carlo simulation to evaluate Equation (18) and Lemma 2 to construct $q\left(\mathbf{x}_{\mathcal{J}_m} | \mathbf{x}_{\mathcal{K}_m}\right)$, is given in Algorithm 2. Algorithm 2 avoids the challenge of estimating high-dimensional densities with kernel density methods by assembling the large densities $q\left(\mathbf{x}_{\mathcal{J}_m}\right)$ and $q\left(\mathbf{x}_{\mathcal{K}_m}\right)$ using the smaller dimensional component densities $q\left(\mathbf{x}_{\mathcal{V}_i}\right)$ and $q\left(\mathbf{x}_{\mathcal{T}_i}\right)$. As a result, the largest dimension estimated with kernel density methods is that of the component with the largest cardinality, $|\mathcal{V}_i|$.

Algorithm 2: Accounting for dependence for inputs to Component m, where $m \geqslant 3$.

Data: Target densities $q\left(\mathbf{x}_{\mathcal{V}_i}\right)$ for $i = 1, \ldots, m-1$ and proposal samples $\left\{\mathbf{x}_{\mathcal{I}_m}^i\right\}_{i=1}^N$.
Result: Target density $q\left(\mathbf{x}_{\mathcal{I}_m}\right)$ evaluated at the proposal samples $\left\{\mathbf{x}_{\mathcal{I}_m}^i\right\}_{i=1}^N$.
for $i = 1 : N$ **do**
  Initialize $q\left(\mathbf{x}_{\mathcal{I}_m}^i\right) = 0$;
  for $s = 1 : S$ **do**
    $\mathbf{x}_{\mathcal{J}_m}^s = \mathbf{x}_{\mathcal{I}_m}^i$.
    for $j = 1 : (m-1)$ **do**
      Generate sample $\mathbf{x}_{\mathcal{V}_j}^s$ from the density $q\left(\mathbf{x}_{\mathcal{V}_j}\right)$ conditioned on the known set $\mathbf{x}_{\mathcal{J}_m}^s$.
      $\mathbf{x}_{\mathcal{J}_m}^s = \mathbf{x}_{\mathcal{J}_m}^s \cup \mathbf{x}_{\mathcal{V}_j}^s$.
    end
    Generate sample $\mathbf{x}_{\mathcal{S}_m}^s$ from $q\left(\mathbf{x}_{\mathcal{S}_m}\right)$ conditioned on the known set $\mathbf{x}_{\mathcal{J}_m}^s$.
    $\mathbf{x}_{\mathcal{J}_m}^s = \mathbf{x}_{\mathcal{J}_m}^s \cup \mathbf{x}_{\mathcal{S}_m}^s$.
    Evaluate $q\left(\mathbf{x}_{\mathcal{I}_m}^i\right) = q\left(\mathbf{x}_{\mathcal{I}_m}^i\right) + \frac{1}{S} q\left(\mathbf{x}_{\mathcal{J}_m}^s\right) / q\left(\mathbf{x}_{\mathcal{K}_m}^s\right)$ using Equation (12);
  end
end

DOI: 10.1002/nme

We note here that for $m = 2$, the input target density may be obtained in a similar fashion to what is carried out in Algorithm 2. In this case, the innermost for-loop is modified so that samples are taken from the target density, $q\left(\mathbf{x}_{\mathcal{V}_1}\right)$, and the new system input density, $q\left(\mathbf{x}_{\mathcal{S}_2}\right)$.

4. CONVERGENCE ANALYSIS & A POSTERIOR INDICATOR

This section addresses the convergence properties of the decomposition-based multicomponent uncertainty analysis approach, describes an *a posteriori* indicator to assess proposal quality, and presents a simple example to demonstrate convergence.

4.1. Convergence

We prove here that the decomposition-based multicomponent uncertainty analysis approach leads to the convergence in distribution of all of the variables associated with a given feed-forward system.

Theorem 1
Let f_m, for $m = 1, 2, \ldots, M$, be the functions comprising an M-component feed-forward system, where the input spaces of the functions can be partitioned such that on each partition, the functions are one-to-one and continuously differentiable. Let the system inputs be absolutely continuous random variables. Then the target random variables for all system variables estimated via the decomposition-based multicomponent uncertainty analysis procedure converge in distribution to their respective true target random variables as the number of samples tends to infinity.

Proof
For each component $m = 1, 2, \ldots, M$, local uncertainty analysis using n samples drawn from the proposal distribution functions, $P\left(\mathbf{x}_{\mathcal{I}_m}\right)$, results in proposal empirical distribution functions, $P^n\left(\mathbf{x}_{\mathcal{I}_m}\right)$. Define the set $\mathcal{M}_1$ as the indices of the components with no dependence on upstream components, $\mathcal{M}_1 = \left\{m \in \{1, 2, \ldots, M\} : \mathcal{I}_m \cap \left(\cup_{i=1}^{M} \mathcal{O}_i\right) = \emptyset\right\}$. The target distribution functions, $Q\left(\mathbf{x}_{\mathcal{I}_m}\right)$, for each component $m \in \mathcal{M}_1$ are therefore known. We estimate the densities $\hat{q}_m\left(\mathbf{x}_{\mathcal{I}_m}\right)$ for $m \in \mathcal{M}_1$ from samples of the target distribution functions using a kernel density estimation method that is strongly uniform convergent [26]. Then, for each $m \in \mathcal{M}_1$,

$$\lim_{n\to\infty} \hat{q}_m\left(\mathbf{x}_{\mathcal{I}_m}\right) = q\left(\mathbf{x}_{\mathcal{I}_m}\right), \tag{19}$$

for all points of continuity of the target density $q\left(\mathbf{x}_{\mathcal{I}_m}\right)$. Because all inputs to the components in the set $\mathcal{M}_1$ are absolutely continuous random variables, the measure of the set of discontinuous points of $q\left(\mathbf{x}_{\mathcal{I}_m}\right)$ is zero. Equation (3) defines the weighted empirical distribution function $Q^n\left(\mathbf{x}_{\mathcal{I}_m}\right)$, and by Lemma 1, we have

$$\lim_{n\to\infty} Q^n\left(\mathbf{x}_{\mathcal{I}_m}\right) = Q\left(\mathbf{x}_{\mathcal{I}_m}\right). \tag{20}$$

Let $\mathcal{Q}_m^n$ be a random variable with distribution function Q^n, and then $\mathcal{Q}_m^n \xrightarrow{d} \mathbf{x}_{\mathcal{I}_m}$. Then, for each set in the partition of the input space of f_m, we have by Skorokhod's representation theorem, $f_m\left(\mathcal{Q}_m^n\right) \xrightarrow{d} f_m\left(\mathbf{x}_{\mathcal{I}_m}\right)$. Because the boundaries of the sets of the partition comprise a set of measure zero, this convergence applies over the complete domain of the function.

Then, by Lemma 2, we can obtain samples from the joint distribution function of the inputs and outputs for all components in $\mathcal{M}_1$. We then define $\mathcal{M}_2$ as the indices of those components with no dependence on upstream components other than those components in $\mathcal{M}_1$. That is, $\mathcal{M}_2 = \{m \in \{1, 2, \ldots, M\} : \mathcal{I}_m \cap (\cup_{i \notin \mathcal{M}_1} \mathcal{O}_i) = \emptyset\}$. The target distribution functions of all inputs for components $m \in \mathcal{M}_2$ are now available; thus, the analysis described previously for $\mathcal{M}_1$ applies to $\mathcal{M}_2$. We proceed by defining in turn $\mathcal{M}_3, \mathcal{M}_4, \ldots, \mathcal{M}_k$, where $\cup_{i=1}^{k} \mathcal{M}_k = \{1, 2, \ldots, M\}$, and obtaining samples from the distribution functions of all of the inputs and outputs for all components in each $\mathcal{M}_i$. From the samples generated for the components with indices in $\mathcal{M}_k$, we can

DOI: 10.1002/nme

construct the empirical distribution function of all system variables. By the strong law of large numbers, this empirical distribution function converges pointwise to the true distribution function of all system variables. □

The rate of convergence of our decomposition-based uncertainty analysis depends on several elements: the rate of convergence of the underlying Monte Carlo sampling, the rate of convergence of the kernel density estimation, and the quality of the proposal distribution functions relative to their corresponding targets. As already discussed in Section 3.2, choosing a good proposal distribution is particularly important for achieving satisfactory convergence rates; a poor choice of proposal can lead to needing a prohibitive number of samples in the offline phase. While one can provide only qualitative guidance for proposal selection as discussed in Section 3.2, Section 4.2 presents a quantitative metric that compares proposal and target distributions for all inputs and coupling variables, thus highlighting *a posteriori* when a poor proposal choice may have compromised accuracy.

We further note here that although we have shown convergence in distribution of all variables associated with a feed-forward system, for many uncertainty analysis tasks, we may care only about statistics such as the mean and variance of a quantity of interest. Generally, if we have a function $f : \mathbb{R}^s \to \mathbb{R}$ that takes random inputs $(\xi_1, \xi_2, \ldots, \xi_s)^T$, we can estimate the mean of $f(\xi_1, \xi_2, \ldots, \xi_s)$ using Monte Carlo simulation as

$$\bar{f} = \frac{1}{n} \sum_{i=1}^{n} f\left(\xi_1^i, \xi_2^i, \ldots, \xi_s^i\right), \tag{21}$$

where $\left(\xi_1^i, \xi_2^i, \ldots, \xi_s^i\right)^T$ is the i^{th} sample realization of the random input to the function. By the strong law of large numbers, $\bar{f} \xrightarrow{a.s.} \mathbb{E}[f(\xi_1, \xi_2, \ldots, \xi_s)]$ as $n \to \infty$. We may use Monte Carlo simulation to estimate other integral quantities, such as the variance, as well, with almost sure convergence guaranteed by the strong law of large numbers. In our decomposition-based approach to uncertainty analysis, if the functions, f_m, corresponding to each component in the feed-forward system are also bounded, then, by an application of Skorokhod's representation theorem (see, e.g., Reference [24]), the estimated mean and variance of any quantities of interest will converge to the true mean and variance. Thus, our decomposition-based multicomponent uncertainty analysis methodology can perform typical uncertainty analysis tasks in a provably convergent manner.

4.2. A posteriori indicator

Selection of an adequate proposal distribution function should use expert opinion and/or previous knowledge from past analyses. However, a poor proposal distribution may detrimentally affect the convergence performance of the distributed uncertainty assessment approach. In the general case, we cannot analyze *a priori* the effects of a given proposal distribution (if we had such information, we would use it to select a better proposal distribution); instead, we use quantitative indicators to determine *a posteriori* if the results are satisfactory.

Drawing from sequential Monte Carlo methods, we evaluate the quality of our proposal distributions once the importance weights are known, using the effective sample size,

$$n_{\text{eff}} = \frac{1}{\sum_{i=1}^{N} \left(w(\mathbf{x}^i)\right)^2}, \tag{22}$$

where $w(\mathbf{x}^i)$ is the importance weight associated to proposal sample $\mathbf{x}^i$ [28–30]. The effective sample size can range in value from $n_{\text{eff}} = 1$ to $n_{\text{eff}} = N$. A value of $n_{\text{eff}} = N$ indicates that the proposal and target distributions are equivalent, while a value of $n_{\text{eff}} = 1$ indicates an extremely poor proposal distribution where only one sample bears any weight in the weighted empirical distribution. The effective sample size is thus a suitable measure of the degeneracy of a given proposal distribution relative to a given target distribution.

To assess the quality of a distributed uncertainty assessment result, we recommend computing the effective sample size for each component once its target distribution is known. If a component's

DOI: 10.1002/nme

effective sample size is below a user-specified threshold, this indicates that sample impoverishment has occurred to a potentially detrimental degree, and we recommend re-evaluating the local uncertainty analysis for that component. Upon completing the local uncertainty analysis of the component in question, the global compatibility step is computed again and the component's new effective sample size is evaluated. In the re-evaluation step, the component's input target distribution can be used in place of the poor proposal distribution—of course, this re-evaluation breaks the strictly offline/online decomposition of our approach, but this recourse is necessary to provide some robustness. The threshold for n_{eff} is a user choice; we investigate its effect with a simple example in the next section. Guidance can also be found in the importance sampling literature [31].

4.3. Convergence example

The following example lays out a step-by-step application of the approach and demonstrates the convergence in distribution for the system shown in Figure 3. The component functions are

$$\begin{aligned} f_1 &: \xi_4 = \xi_1 + \xi_2 \\ f_2 &: \xi_5 = \xi_2 + \xi_3 \\ f_3 &: \xi_6 = \xi_4 + \xi_5. \end{aligned}$$

The first phase of the approach is to conduct the offline analysis for each local component, which requires selecting proposal distributions for each component's inputs. In this example, the proposal distributions selected are Gaussian with conservative variance estimates. For Component 1, we use $\xi_1 \sim \mathcal{N}(-0.5, 1.5)$ and $\xi_2 \sim \mathcal{N}(1.5, 2.0)$. For Component 2, we use $\xi_2 \sim \mathcal{N}(-1.0, 2.5)$ and $\xi_3 \sim \mathcal{N}(-0.5, 2.5)$. For Component 3, we use $\xi_4 \sim \mathcal{N}(1.5, 5.0)$ and $\xi_5 \sim \mathcal{N}(-1.5, 4.5)$. (Note that the proposal distribution for ξ_2 in the local analysis for Component 1 is not necessarily the same as the proposal distribution for ξ_2 in the local analysis for Component 2.) Based on these proposal distributions, we conduct a local uncertainty analysis for each of the three components. In each case, we use a Monte Carlo simulation with n ranging from 100 to 1000 samples. Each Monte Carlo simulation results in a set of samples of the component outputs (ξ_4 for Component 1, ξ_5 for Component 2, and ξ_6 for Component 3). For each component, we store the input and output sample datasets.

The next phase of the approach is the online analysis, which uses those samples pre-computed in the offline phase and does not require additional evaluations of any of the components. The first step in the online analysis is to specify target distributions for all system inputs, in this case ξ_1, ξ_2, and ξ_3. These target distributions represent the particular scenario for which we wish to analyze the system. In this example, we specify all three system inputs to have standard Gaussian distributions: $\xi_1 \sim \mathcal{N}(0, 1), \xi_2 \sim \mathcal{N}(0, 1)$, and $\xi_3 \sim \mathcal{N}(0, 1)$. We then begin with the upstream components, here Component 1 and Component 2. Given the newly specified target distributions and the proposal distributions assumed in the offline phase, for each component, we compute the importance weights using Algorithm 1. We apply these importance weights to the corresponding samples of component outputs, here ξ_4 and ξ_5. This gives updated estimates of the component output distributions. The next step is to resolve the dependence structure between ξ_4 and ξ_5, induced by the shared input variable ξ_2. We achieve this using Algorithm 2, which evaluates the joint target density $q(\xi_4, \xi_5)$ at the input proposal samples of Component 3. The last step of the online phase is to compute the importance weights for Component 3, using the newly acquired target density $q(\xi_4, \xi_5)$ evaluations from Algorithm 2. Applying these importance weights to the pre-computed samples of ξ_6 leads to the final updated estimate of the system output.

For this particular scenario, we can compute the true system output distribution analytically as a Gaussian distribution, $\xi_6 \sim \mathcal{N}(0, 6)$. We compare the numerical results from our decomposition approach to this analytical solution. The convergence in distribution is demonstrated with the Cramer von-Mises criterion,

$$\omega = \int_{-\infty}^{\infty} \left(\Pi^n(\xi_6) - \Pi(\xi_6)\right)^2 \, \mathrm{d}\Pi(\xi_6), \tag{23}$$

DOI: 10.1002/nme

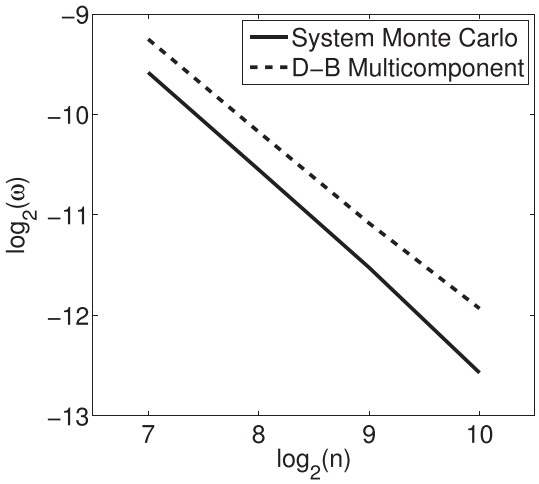

Figure 5. The results indicate the output of interest, ξ_6; Cramer von-Mises criterion converges with the number of samples.

where $\Pi^n(\xi_6)$ and $\Pi(\xi_6)$ are the empirical and analytical distribution functions of ξ_6, respectively. The Cramer von-Mises criterion is estimated using Monte Carlo simulation, where samples of ξ_6 are drawn from the analytical distribution $\Pi(\xi_6)$.

Figure 5 presents the averages over 100 independent simulations of an all-at-once system Monte Carlo uncertainty analysis and our decomposition-based approach. The decomposition-based results implemented the kernel density estimation method and used 25 samples, S, to resolve the dependence among variables in Algorithm 2. The result shows that for the same number of overall samples per component, n, we incur a larger error than the system-level Monte Carlo simulation. This error is due to Algorithm 1. Specifically, the target measure needs to be absolutely continuous with respect to the proposal measure, which leads to a conservative choice of proposal density. This in turn means that there exist proposal samples that have negligible importance weight ('wasted' samples). The closer the proposal distribution to the target distribution, the smaller this offset. This is the price we pay for decomposition—it is important to emphasize that our goal is not an improvement in computational efficiency, but rather the ability to manage system complexity and to analyze uncertainty in systems for which an integrated Monte Carlo simulation approach may not be tractable or feasible. Furthermore, our approach can perform the local uncertainty analysis of each component concurrently. This could lead to significant further run time improvement compared to the system Monte Carlo uncertainty analysis, which can perform uncertainty analysis on downstream models only after their respective dependent upstream components' uncertainty analyses are complete.

Figure 6 demonstrates the effects of changing the proposal distribution on the convergence of the decomposition-based approach for this simple example. Here, we consider modifying the proposal distribution of Component 2 while keeping the proposal distributions of Component 1 and Component 3 the same as the previous analysis, with $n = 256$. The proposal distribution for Component 2 is a bivariate Gaussian distribution with zero mean and diagonal variance set to 1.5, 3.0, 6.0, and 12.0 representing a degradation of the proposal distribution. These four cases result, respectively, in values of $n_{\text{eff}} = 220, 140, 75$, and 40. As the proposal distribution improves, the ratio n_{eff}/n increases (for this example n is fixed), which in turn leads to improved estimation of the outputs of interest as shown by the decreasing Cramer von-Mises criterion in Figure 6.

5. RESULTS

In this section, we present a demonstration of the decomposition-based multicomponent uncertainty analysis approach for a gas turbine blade application. We compare the results of our method with all-at-once Monte Carlo system uncertainty analysis.

DOI: 10.1002/nme

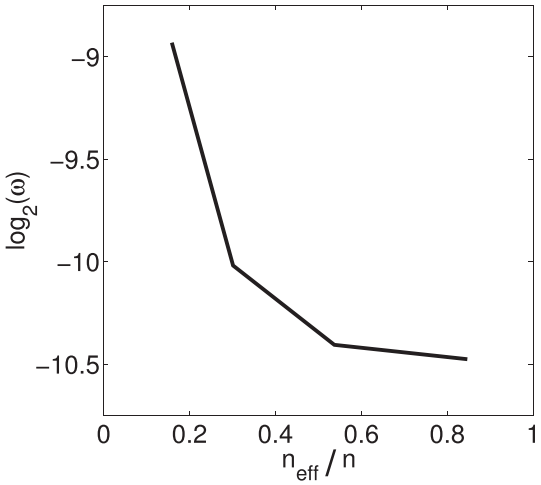

Figure 6. The results show the implications of selecting a poor proposal distribution for component f_2 with $n = 256$. As n_{eff} approaches n, indicating a better proposal distribution, the accuracy of our estimate improves.

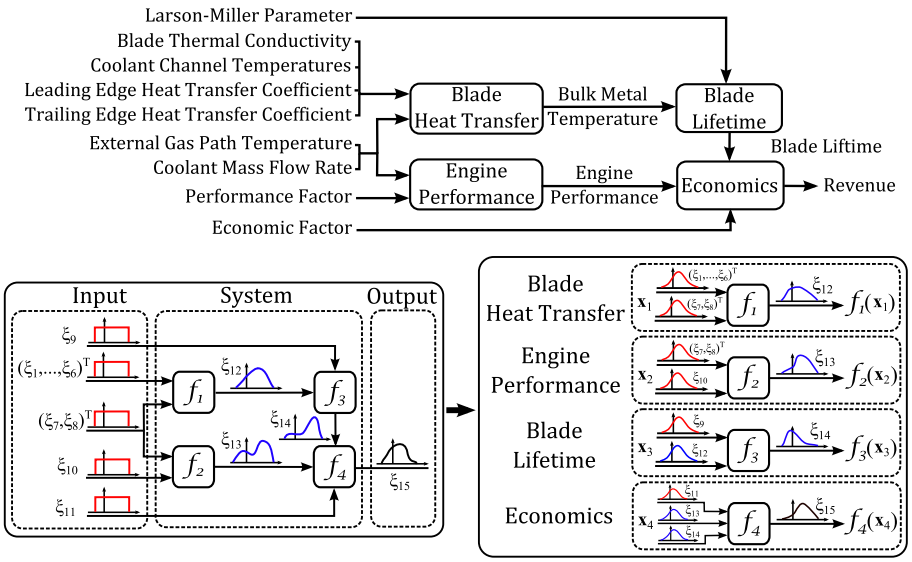

Figure 7. The gas turbine application problem contains four components, each representing a disciplinary analysis: heat transfer, structures, performance, and economics.

5.1. Application

Our application problem consists of four components, each representing a disciplinary analysis: blade heat transfer, blade lifetime, engine performance, and an economic model. The functional relationships and random variables are shown in Figure 7. This application is representative of an organizational multidisciplinary environment where different groups are responsible for different aspects of the gas turbine design and assessment. The specific objective of our analysis is to quantify the effects of uncertainties throughout the gas turbine design process on the output of interest, here the economics of the product. We consider the uncertain system inputs shown in Table II. The distributions shown in the table are the target distributions used for our analysis (i.e., they represent the particular scenario of interest in the system uncertainty analysis). These target distributions are considered unknown when conducting the local uncertainty analysis for each of the four components.

DOI: 10.1002/nme

Table II. Gas turbine system input uncertainty distributions where $\mathcal{U}(a, b)$ represents a uniform distribution between the lower limit a and upper limit b.

Variable	Name	Description	Units	Distribution
ξ_1	T_{c1}	First passage coolant temperature	K	$\mathcal{U}(590, 610)$
ξ_2	T_{c2}	Second passage coolant temperature	K	$\mathcal{U}(640, 660)$
ξ_3	T_{c3}	Third passage coolant temperature	K	$\mathcal{U}(690, 710)$
ξ_4	k	Blade thermal conductivity	W/m/K	$\mathcal{U}(29, 31)$
ξ_5	h_{LE}	Leading edge heat transfer coefficient	W/m^2/K	$\mathcal{U}(1975, 2025)$
ξ_6	h_{TE}	Trailing edge heat transfer coefficient	W/m^2/K	$\mathcal{U}(975, 1025)$
ξ_7	$\dot{m}$	Coolant mass flow rate	kg/sec	$\mathcal{U}(0.108, 0.132)$
ξ_8	T_g	External gas path temperature	K	$\mathcal{U}(1225, 1275)$
ξ_9	LMP	Larson–Miller parameter	–	$\mathcal{U}(2.45 \cdot 10^4, 2.55 \cdot 10^4)$
ξ_{10}	F_{perf}	Performance factor	–	$\mathcal{U}(0.85, 0.95)$
ξ_{11}	F_{econ}	Economic factor	–	$\mathcal{U}(0.9, 1.1)$

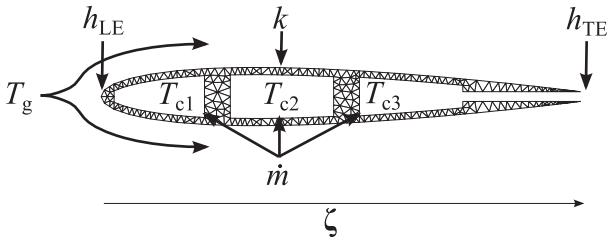

Figure 8. The gas turbine blade profile and mesh, along with the random input variables.

Table III. Heat transfer model input proposal uncertainty distributions.

Variable	Name	Description	Units	Distribution
ξ_1	T_{c1}	First passage coolant temperature	K	$\mathcal{N}(595, 75)$
ξ_2	T_{c2}	Second passage coolant temperature	K	$\mathcal{N}(645, 75)$
ξ_3	T_{c3}	Third passage coolant temperature	K	$\mathcal{N}(705, 75)$
ξ_4	k	Blade thermal conductivity	W/m/K	$\mathcal{N}(29, 1.5)$
ξ_5	h_{LE}	Leading edge heat transfer coefficient	W/m^2/K	$\mathcal{N}(2025, 1500)$
ξ_6	h_{TE}	Trailing edge heat transfer coefficient	W/m^2/K	$\mathcal{N}(1000, 500)$
ξ_7	$\dot{m}$	Coolant mass flow rate	kg/sec	$\mathcal{N}(0.12, 10^{-4})$
ξ_8	T_g	External gas path temperature	K	$\mathcal{N}(1260, 450)$

Heat Transfer Model. The blade heat transfer model simulates a cooled gas turbine blade in hot gas path flow using finite element analysis. The uncertain inputs to this subsystem are shown in Figure 7. We consider three blade passages, each with its own independent coolant temperature variable. Thus, there are eight uncertain inputs to this component. External heat transfer along the pressure and suction side surfaces is computed as

$$htc(\zeta) = h_{TE} + (h_{LE} - h_{TE}) \cdot exp\left(-4 \cdot \left(\frac{\zeta}{c}\right)^2\right), \tag{24}$$

where ζ is the chordwise spatial coordinate and c is the blade chord length, here taken as $c = 0.04$ [m]. The output of the heat transfer model is bulk metal temperature, T_{bulk} [K]. The relationship between the input and output variables is computed using a finite element method to solve the heat equation. The blade profile and mesh along with the random variables are shown in Figure 8.

The local uncertainty analysis for this model is conducted using the proposal distributions shown in Table III. Note that for our particular demonstration, we have chosen the proposal variances conservatively to ensure adequate support in the proposal samples, as discussed in Section 3.3.

DOI: 10.1002/nme

Lifetime Model. The lifetime model estimates the expected time until blade failure assuming a Larson–Miller [32] nickel super alloy stress-to-failure scenario. As shown in Figure 7, the inputs to this subsystem are bulk temperature, T_{bulk}, and the Larson–Miller failure parameter, LMP. The output is expected time until failure, t_{fail} [h]. The relationship between the input and output variables is given by

$$t_{fail} = exp\left(\frac{LMP}{T_{bulk}} - 20\right). \tag{25}$$

The input proposal distributions assumed for the local uncertainty analysis of this component are given in Table IV.

Performance Model. A high-fidelity gas turbine performance model would account for compressor coolant flow extraction, leakage losses, and mixing losses, which is beyond the scope of this work. Instead, a simplified low-fidelity model is implemented to evaluate the maximum power. The performance model rewards high external hot gas path temperatures and penalizes coolant flow usage. As shown in Figure 7, the inputs to this subsystem are external gas temperature, T_{gas}, performance factor, F_{perf}, and coolant mass flow, $\dot{m}$. The performance factor, F_{perf}, is introduced to account for the effects on engine performance of randomness associated with other gas turbine components. The output of the performance model is engine performance, P_{eng}, defined as

$$P_{eng} = F_{perf} \cdot (\dot{m}_o - N \cdot \dot{m}) \cdot C_p \cdot T_o \cdot \left(\frac{T_g}{T_o} - 2 \cdot \sqrt{\frac{T_g}{T_o}} + 1\right), \tag{26}$$

where T_o is the inlet compressor temperature, $\dot{m}_o$ is the inlet compressor flow rate, N is the number of gas turbine blades, and C_p is the specific heat at constant pressure. These parameters are treated deterministically and set to the values $T_o = 300$ [K], $\dot{m}_o = 430$ [kg/s], $N = 90$, and $C_p = 1003.5$ [J/kg/K]. The input proposal distributions assumed for the local uncertainty analysis of this component are given in Table V.

Economics Model. The economics model simulates the revenue from the operating gas turbine. The model rewards a high-performance gas turbine engine and penalizes a gas turbine engine that introduces risk of failure. As shown in Figure 7, the inputs to this subsystem are expected time until failure, t_{fail}, engine performance, P_{eng}, and economic factor, F_{econ}. The economic factor, F_{econ}, is introduced to account for randomness associated with other gas turbine components not represented in the models. The output is revenue, r_{econ}, defined as

$$r_{econ} = F_{econ} \cdot t_{fail} \cdot P_{eng} \cdot c_o, \tag{27}$$

Table IV. Blade lifetime model input proposal uncertainty distributions.

Variable	Name	Description	Units	Distribution
ξ_{10}	LMP	Larson–Miller parameter	–	$\mathcal{N}(2.5 \cdot 10^4, 2 \cdot 10^5)$
ξ_{12}	T_{bulk}	Bulk metal temperature	K	$\mathcal{N}(865, 400)$

Table V. Performance model input proposal uncertainty distributions.

Variable	Name	Description	Units	Distribution
ξ_7	$\dot{m}$	Coolant mass flow rate	kg/sec	$\mathcal{N}(0.115, 10^{-4})$
ξ_8	T_g	External gas path temperature	K	$\mathcal{N}(1240, 500)$
ξ_{10}	F_{perf}	Performance factor	–	$\mathcal{N}(0.9, 7.5 \cdot 10^{-3})$

DOI: 10.1002/nme

Table VI. Economics model input proposal uncertainty distributions.

Variable	Name	Description	Units	Distribution
ξ_{11}	F_{econ}	Economic factor	–	$\mathcal{N}(1.0, 0.01)$
ξ_{13}	t_{fail}	Blade lifetime	year	$\mathcal{N}(425, 6 \cdot 10^4)$
ξ_{14}	P_{eng}	Engine performance	MW	$\mathcal{N}(120, 150)$

where c_o is the cost of energy, which is treated deterministically and set to the value $c_o = 0.07$ [\$/kWh]. The input proposal distributions assumed for the local uncertainty analysis of this component are given in Table VI.

Multicomponent Uncertainty Analysis Results. In the 'offline phase', the local uncertainty analyses are carried out for each component individually, using the input proposal distributions specified in Tables III–VI. Each component uses n independent samples in its local Monte Carlo simulation. (Note that the number of samples does not need to be the same across components.) Output samples for each component are stored in a database.

The 'online phase' considers a system uncertainty analysis for the system input distributions shown in Table II. Global compatibility satisfaction begins by considering the Heat Transfer and Performance components, which have only system inputs and thus require no information from upstream disciplines. Using Algorithm 1 and kernel density estimation, we obtain target densities $q(\xi_{12}, \xi_7, \xi_8)$ and $q(\xi_{13}, \xi_7, \xi_8)$. The same procedure is applied to the Lifetime component using the recently acquired density $q(\xi_{12})$ to obtain the target density $q(\xi_{14}, \xi_{12})$. Using target densities $q(\xi_{12}, \xi_7, \xi_8)$, $q(\xi_{13}, \xi_7, \xi_8)$, and $q(\xi_{14}, \xi_{12})$ along with Algorithm 2 with $S = 200$ samples, we obtain the desired target density $q(\xi_{13}, \xi_{14})$ evaluated at the Economic model's proposal samples. The global compatibility satisfaction procedure is then performed on the Economics model to obtain the system output of interest, revenue, with target density $q(\xi_{15})$. The Cramer von-Mises convergence plots for variables ξ_{12}, ξ_{13}, ξ_{14}, and ξ_{15} averaged over 100 independent simulations are shown in Figure 9. The true distribution is defined by the empirical distribution function generated using a system Monte Carlo simulation with 10^6 samples.

The system output of interest distribution function using the decomposition-based uncertainty analysis approach is given in Figure 10. For comparison, the proposal distribution function and the system Monte Carlo uncertainty analysis distribution function are also shown in Figure 10. The results show that the decomposition-based approach propagated, in the online phase, the target system input uncertainty distributions through the system to obtain an adequate representation of the system output of interest distribution. We emphasize that this online phase required no additional evaluations of any of the component models. Our decomposition-based approach therefore provides a quantitative means of calculating the system output of interest relevant statistics and failure probabilities.

The small discrepancy between the decomposition-based uncertainty analysis approach and the system Monte Carlo uncertainty analysis approach is due to the errors introduced by the finite number of samples used in the density estimation step, the Monte Carlo approximation used in Algorithm 2, and the sample impoverishment introduced by the requirement that target distributions be absolutely continuous with respect to their proposal distributions. The sample impoverishment error can be minimized by using more appropriate proposal distributions. However, it is not always possible to correctly predict the range of the target distribution. This is one of the prices to pay for decomposition.

Flexibility of the Decomposition-Based Multicomponent Uncertainty Analysis. A benefit of our decomposition-based approach is that if any system input distributions are modified, yet remain absolutely continuous with respect to their proposal distribution, then the system output of interest distribution function can be re-computed with no additional component analyses. For example, if the system input variables ξ_5, ξ_6, ξ_8, and ξ_9 are modified from those in Table II to those in Table VII, then the results given by the system Monte Carlo uncertainty analysis are invalid. However, our decomposition-based approach can, with no additional evaluations of any of the component models, evaluate the system output of interest distribution function

DOI: 10.1002/nme

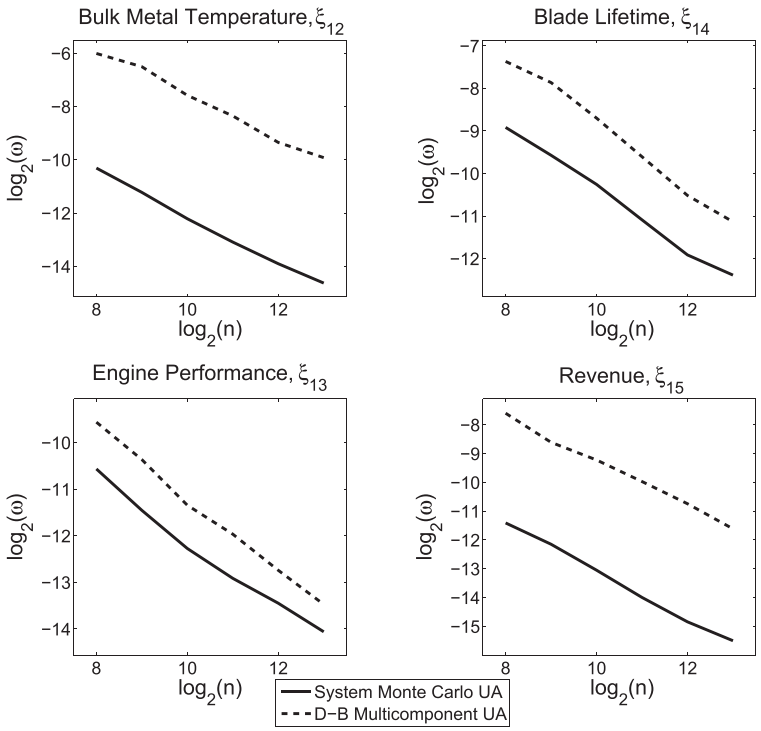

Figure 9. The Cramer von-Mises convergence plots are shown for the intermediate variables ξ_{12}, ξ_{13}, and ξ_{14} as well as for the system output of interest, revenue, ξ_{15}. The solid lines are the results obtained from a system Monte Carlo simulation. The dashed lines are the results obtained using our decomposition-based multicomponent uncertainty analysis.

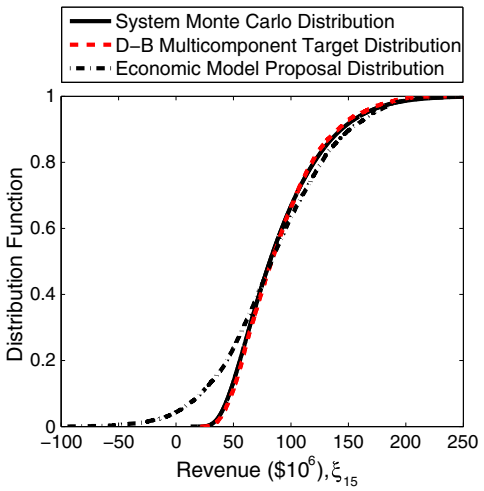

Figure 10. The system output of interest, revenue, distribution function using $n = 8192$ samples is shown in millions of dollars. The solid line is the result obtained from a system Monte Carlo simulation. The dashed line is the result obtained from the decomposition-based multicomponent uncertainty analysis. The dash-dot line is the result obtained from the local uncertainty analysis of the Economics model.

as shown in Figure 11. For comparison, the previous system Monte Carlo uncertainty analysis distribution function and a new system Monte Carlo uncertainty analysis distribution function, which required evaluating the entire system again, are also shown in Figure 11. The results show the decomposition-based approach, without re-evaluating any component, approximated the distribution function accurately.

DOI: 10.1002/nme

Table VII. Updated gas turbine system input uncertainty distributions.

Variable	Name	Description	Units	Distribution
ξ_5	h_{LE}	Leading edge heat transfer coefficient	W/m^2/K	$\mathcal{U}(2025, 2075)$
ξ_8	T_g	External gas path temperature	K	$\mathcal{U}(1240, 1280)$
ξ_9	LMP	Larson–Miller parameter	–	$\mathcal{U}(2.425 \cdot 10^4, 2.525 \cdot 10^4)$

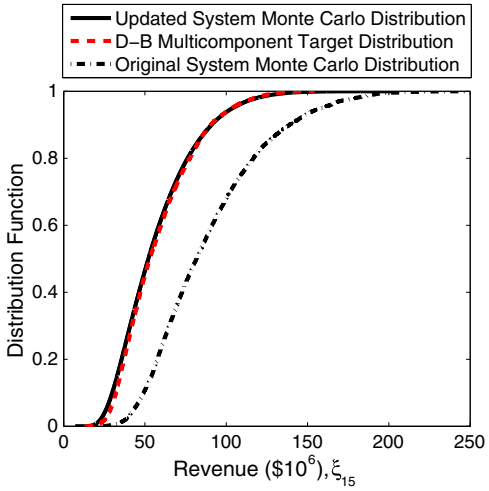

Figure 11. The system output of interest, revenue, distribution function using $n = 8192$ samples is shown in millions of dollars. The solid line is the result obtained from an updated system Monte Carlo simulation, which required evaluating the entire system again. The dashed line is the result obtained from the decomposition-based multicomponent uncertainty analysis using the online phase only. The dash-dot line is the result from the previous Monte Carlo uncertainty analysis.

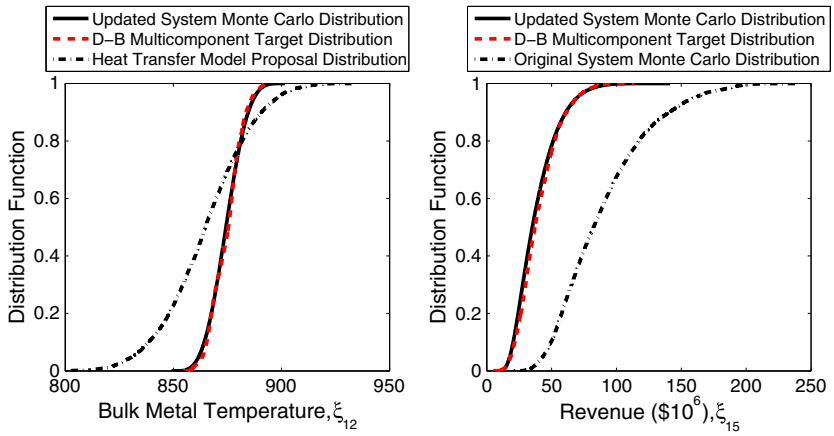

Figure 12. The bulk metal temperature, ξ_{12}, is shown on the left. The results shows that the proposal distribution (dash-dot line) of the bulk metal temperature of the Lifetime model supports the target distribution (dashed line) coming from the Heat Transfer model. The system Monte Carlo uncertainty analysis results, solid line, required evaluating the Heat Transfer, Lifetime, and Economics model, whereas the decomposition-based multicomponent uncertainty analysis results were obtained using the online phase only. The revenue, ξ_{15}, in millions of dollars is shown on the right. The solid line is the result obtained from a system Monte Carlo uncertainty analysis. The dashed line is the result obtained from the decomposition-based multicomponent uncertainty analysis using the online phase only. The dash-dot line is the result obtained from the previous Monte Carlo uncertainty analysis.

DOI: 10.1002/nme

Likewise, a modification to a component would require the system Monte Carlo uncertainty analysis approach to recompute the samples associated with the modified component and any components that depend on the modified component. In contrast, our decomposition-based uncertainty analysis approach would only have to perform the local uncertainty analysis on the modified component and those components for which the target distribution is no longer absolutely continuous with respect to the proposal distribution. For example, if the Heat Transfer component modified the heat transfer enhancement in the cooling channels from a factor of 2.5 to 2.25, then the target density $q(\xi_{12})$ would still be absolutely continuous with respect to the Lifetime model proposal density $p(\xi_{12})$ as shown in Figure 12. As a result, the decomposition-based approach would not require the Lifetime model or the Economics model to perform a local uncertainty analysis whereas the system Monte Carlo uncertainty analysis approach would. Instead, the decomposition-based approach evaluates the system output of interest distribution shown in Figure 12 using only the online phase.

6. CONCLUSION

This paper has presented a new decomposition-based approach to uncertainty analysis of complex multicomponent systems. The approach is motivated by the advantages brought about by decomposition: managing complexity through a divide-and-conquer strategy, exploiting specific disciplinary expertise through local analyses, promoting disciplinary/component autonomy while maintaining an awareness of system-level issues, and being consistent with many organizational structures. These are essential characteristics to achieve a sustainable strategy that manages uncertainty in the complex settings of today's modern engineered systems.

These characteristics are emphasized by drawing analogies between our decomposition approach to uncertainty analysis and decomposition-based strategies for multidisciplinary optimization. In the multidisciplinary optimization literature, approaches are often categorized as monolithic versus distributed, and open consistency versus closed consistency [33–35]. Our approach has a distributed architecture, that is, the system uncertainty analysis is partitioned into multiple uncertainty analyses. This is in contrast to a monolithic architecture, which solves the problem in its entirety. Our approach has open consistency, that is, our samples are initially observations from the incorrect probability distributions but upon convergence become consistent with the desired distributions. In contrast, a closed consistency formulation requires that each sample satisfies global compatibility constraints at every stage of the algorithm.

This paper has focused on a method for the forward propagation of uncertainties through a feed-forward system. Further research is required to extend the general idea to systems with two-way coupling and/or feedback loops. Such systems will require iteration between components in the online phase, thus destroying the clean partition between offline and online phases that we achieve in the feed-forward case. Despite this drawback, the decomposition can still realize many of the advantages discussed in the introduction. A further limitation is that the current approach has been presented only for systems with random variables and random vectors. An important area of future work is to extend the method to systems that include random fields. This will require drawing on recent work to couple Karhunen-Loève expansion representations of random fields [14–16]. Lastly, we note that the examples studied demonstrate the promise of the decomposition-based approach; however, future work must also address the challenges of scalability. In particular, the density estimation step (required to estimate importance weights) currently limits the number of dependent variables that can be considered.

ACKNOWLEDGEMENTS

This work was supported in part by the International Design Center at the Singapore University of Technology and Design, by the DARPA META program through AFRL Contract FA8650-10-C-7083 and Vanderbilt University Contract VU-DSR#21807-S7, and by the US Federal Aviation

DOI: 10.1002/nme

Administration Office of Environment and Energy under FAA Award No. 09-C-NE-MIT, Amendment Nos. 028, 033, and 038, managed by Rhett Jefferies and James Skalecky, FAA. Any opinions, findings, and conclusions or recommendations expressed in this material are those of the authors and do not necessarily reflect the views of the FAA.

REFERENCES

1. Braun RD, Kroo IM. Development and Application of the Collaborative Optimization Architecture in a Multidisciplinary. *Multidisciplinary Design Optimization: State of the Art* 1997; **80**:98–116.
2. Kroo I. Distributed multidisciplinary design and collaborative optimization. *VKI Lecture Series on Optimization Methods & Tools for Multicriteria/Multidisciplinary Design*, Sint-Genesius-Rode, Belgium, Unknown Month November 15; 1–22.
3. Sobieszczanski-Sobieski J, Agte J, Sandusky R. Bilevel integrated system synthesis. *AIAA Journal* 2000; **38**(1): 164–172.
4. Kim HM, Michelena N, Papalambros P, Jiang T. Target cascading in optimal system design. *Journal of Mechanical Design* 2003; **125**(3):474–480.
5. Martin J, Simpson T. A methodology to manage system-level uncertainty during conceptual design. *Journal of Mechanical Design* 2006; **128**(4):959–968.
6. Yao W, Chen X, Luo W, van Tooren M, Guo J. Review of uncertainty-based multidisciplinary design optimization methods for aerospace vehicles. *Progress in Aerospace Sciences* 2011; **47**(6):450–479.
7. Gu XS, Renaud J, Penninger C. Implicit uncertainty propagation for robust collaborative optimization. *Journal of Mechanical Design* 2006; **128**(4):1001–1013.
8. Chiralaksanakul A, Mahadevan S. Decoupled approach to multidisciplinary design optimization under uncertainty. *Optimization and Engineering* 2007; **8**(1):21–42.
9. McDonald M, Zaman K, Mahadevan S. Uncertainty quantification and propagation for multidisciplinary system analysis. *12th AIAA/ISSMO Multidisciplinary Analysis and optimization Conference, Paper 2008-6038*, Victoria, BC, Canada, 2008; 1-12.
10. Kokkolaras M, Mourelatos ZP, Papalambros PY. Design optimization of hierarchically decomposed multilevel systems under uncertainty. *Journal of Mechanical Design* 2006; **128**(2):503–508.
11. Du X, Chen W. Collaborative reliability analysis under the framework of multidisciplinary systems design. *Optimization and Engineering* 2005; **6**(1):63–84.
12. Mahadevan S, Smith N. Efficient first-order reliability analysis of multidisciplinary systems. *International Journal of Reliability and Safety* 2006; **1**(1):137–154.
13. Sankararaman S, Mahadevan S. Likelihood-based approach to multidisciplinary analysis under uncertainty. *Journal of Mechanical Design* 2012; **134**(3):031008, 1–12.
14. Arnst M, Ghanem R, Phipps E, Red-Horse J. Dimension reduction in stochastic modeling of coupled problems. *International Journal for Numerical Methods in Engineering* 2012; **92**(11):940–968.
15. Arnst M, Ghanem R, Phipps E, Red-Horse J. Measure transformation and efficient quadrature in reduced-dimensional stochastic modeling of coupled problems. *International Journal for Numerical Methods in Engineering* 2012; **92**(12):1044–1080.
16. Arnst M, Ghanem R, Phipps E, Red-Horse J. Reduced chaos expansions with random coefficientsin reduced-dimensional stochastic modeling of coupled problems. *International Journal for Numerical Methods in Engineering* 2014; **97**(5):352–376.
17. Constantine P, Phipps E, Wildey TM. Efficient uncertainty propagation for network multiphysics systems. *International Journal for Numerical Methods in Engineering* 2014; **99**(3):183–202. doi:10.1002/nme.4667.
18. Arnst M, Craig S, Ghanem R. Hybrid sampling/spectral method for solving stochastic coupled problems. *SIAM/ASA Journal on Uncertainty Quantification* 2013; **1**(1):218–243.
19. Chen X, Ng B, Sun Y, Tong C. A flexible uncertainty quantification method for linearly coupled multi-physics systems. *Journal of Computational Physics* 2013; **248**(1):383–401.
20. Jakeman J, Eldred M, Xiu D. Numerical approach for quantification of epistemic uncertainty. *Journal of Computational Physics* 2010; **229**(12):4648–4663.
21. Chen X, Park EJ, Xiu D. A flexible numerical approach for quantification of epistemic uncertainty. *Journal of Computational Physics* 2013; **240**(1):211–224.
22. Cacuci D. *Sensitivity and Uncertainty Analysis: Theory*, Sensitivity and Uncertainty Analysis. Chapman & Hall/CRC: Boca Raton, Florida, 2003.
23. Smith A, Gelfand A. Bayesian statistics without tears: a sampling–resampling perspective. *The American Statistician* 1992; **46**(2):84–88.
24. Grimmett G, Stirzaker D. *Probability and Random Processes*, Texts from Oxford University Press. Oxford University Press: New York, 2001.
25. Parzen E. On estimation of a probability density function and mode. *The Annals of Mathematical Statistics* 1962; **33**(3):1065–1076.
26. Devroye L, Penrod CS. The strong uniform convergence of multivariate variable kernel estimates. *Canadian Journal of Statistics* 1986; **14**(3):211–220.

DOI: 10.1002/nme

27. Hall P, Sheather S, Jones M, Marron J. On optimal data-based bandwidth selection in kernel density estimation. *Biometrika* 1991; **78**(2):263–269.
28. Kong A, Liu J, Wong W. Sequential imputations and bayesian missing data problems. *Journal of the American Statistical Association* 1994; **89**(425):278–288.
29. Liu J. Metropolized independent sampling with comparisons to rejection sampling and importance sampling. *Statistics and Computing* 1996; **6**(2):113–119.
30. Doucet A, Godsill S, Andrieu C. On sequential monte carlo sampling methods for bayesian filtering. *Statistics and Computing* 2000; **10**(3):197–208.
31. Lenth R. Some practical guidelines for effective sample size determination. *The American Statistician* 2001; **55**(3):187–193.
32. Reed RC. *The Superalloys: Fundamentals and applications*. Cambridge University Press: New York, 2006.
33. Alexandrov NM, Hussaini Y. *Multidisciplinary Design Optimization: State of the Art*, Proceedings in Applied Mathematics Series; No. 80. Society for Industrial and Applied Mathematics: Philadelphia, PA, 1997.
34. Alexandrov N, Lewis R. Algorithmic perspectives on problem formulations in MDO. *AIAA Paper 2000-4719, 8th AIAA/USAF/NASA/ISSMO Symposium on Multidisciplinary Analysis and Optimization*, Long Beach, CA, 6–8 September 2000.
35. Cramer E, Dennis Jr, J, Frank P, Lewis RM, Shubin G. Problem formulation for multidisciplinary optimization. *SIAM Journal on Optimization* 1994; **4**(4):754–776.

DOI: 10.1002/nme